International Journal of Physical Sciences

ABOUT IJPS

The **International Journal of Physical Sciences (IJPS)** is published weekly (one volume per year) by Academic Journals.

International Journal of Physical Sciences (IJPS) is an open access journal that publishes high-quality solicited and unsolicited articles, in English, in all Physics and chemistry including artificial intelligence, neural processing, nuclear and particle physics, geophysics, physics in medicine and biology, plasma physics, semiconductor science and technology, wireless and optical communications, materials science, energy and fuels, environmental science and technology, combinatorial chemistry, natural products, molecular therapeutics, geochemistry, cement and concrete research, metallurgy, crystallography and computer-aided materials design. All articles published in IJPS are peer-reviewed.

Contact Us

International Journal of Physical Sciences

ARTICLES

Full Length Research Paper

Problems with p⁶Li plasma in a fusion reactor

J. Bahmani*, B. Eslami and F. Mohammad Jafari

Department of Physics, Payam Noor University, Tehran, Iran.

Problems of using proton-Lithium-6 (p⁶Li) fuel are energy losses that occur in a fusion reactor. Investigating the energy balance equation in this fuel is significant. The p⁶Li reaction is termed aneutronic, as it produces relatively few neutrons and requires none for breeding. The energy from the charged reaction products can be directly converted to electrical power at a much higher efficiency than Deuterium-tritium (DT). In this paper, the approach of optimum performance of p⁶Li fuel in fusion reactors was presented investigating the energy balance equations for ions and electrons. The optimum fuel mixture is almost $\frac{n_p}{n_{6_{Li}}} = 3$. The performance was determined to be p⁶Li and is favorable for Ti=800 keV.

Key words: Fuel, reactor, energy, radiation.

INTRODUCTION

Choice of suitable fuel for fusion reactors is subject to several conditions especially in terms of economic, safety and environmental parameters, while it is very difficult to satisfy all of them. Risks resulting from the release of radioactive materials run as a result of activation of equipment and presence of tritium in the plasma system. Each fusion plasma Deuterium-tritium (DT) releases 17.6 MeV which turn into a kinetic energy with 3.5 MeV helium and 14.1 MeV neutron (Yu and Yu, 2009).

$$_{1}^{2}D + _{1}^{3}T \rightarrow _{2}^{4}He(3.5 \text{ MeV}) + n(14.1 \text{MeV}) \qquad (1)$$
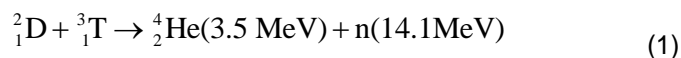
DT reaction has two major disadvantages: (1) It hurts the reactor equipments due to the production of neutron, (2)

reproduction of tritium has more problem and it produces a radial space resulting from blanket of lithium (Stott, 2005). The deuteron-deuteron (DD) fusion plasmas are very attractive since deuterium is abundant and it eliminates the need for breed tritium. The produced neutrons are not a lot and they have less energy than DT plasma. However, there is atmospheric pollution due to tritium production through DD fusion plasmas. D³He plasma is called aneutronic which produces relatively few neutrons and nothing is needed for breeding. Energy resulted from the charged products can directly change into the electric power in a much higher efficiency than DT. Thus, to do the same radioactivity as the DT, higher temperatures 50 to 100 keV are needed. In general, one of the most important alternatives in future fusion reactors
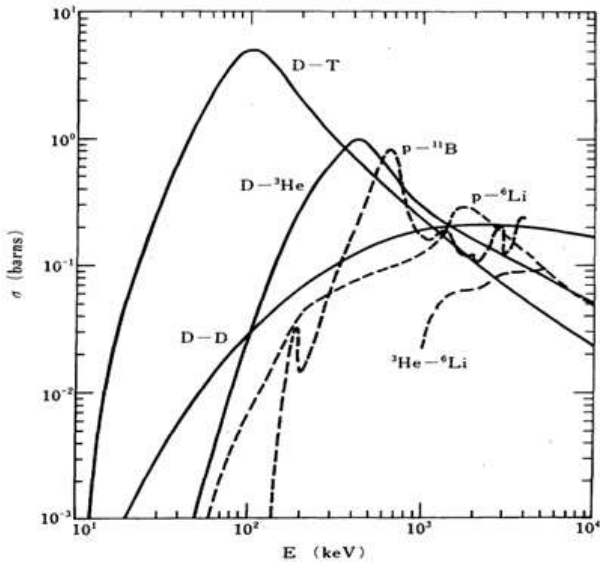
Figure 1. Cross -section as a function of energy for different plasmas (Momota et al., 1980).
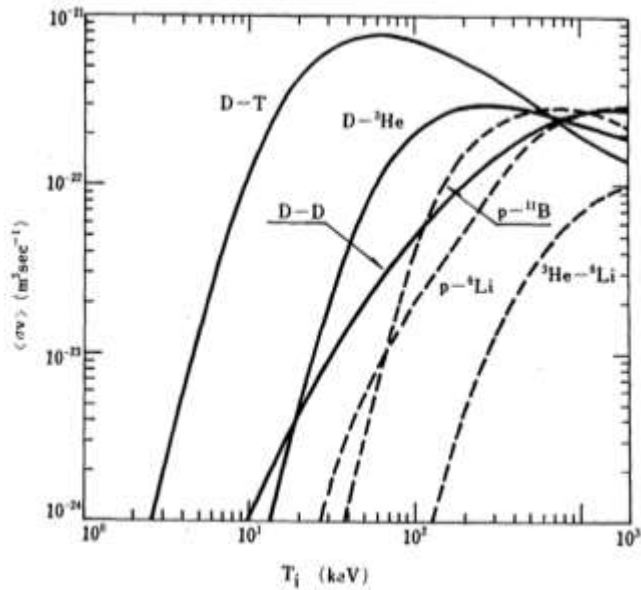
Figure 2. Average reactivity as a function of ion temperature for different plasmas (Momota et al., 1980).

is D^{3}He plasma.

$$_1^2D + _2^3He \rightarrow _2^4He(3.6MeV) + _1^1H(14.7 \text{ MeV}) \quad (2)$$
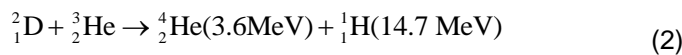
However, the share of "cleanless" has not been done in D^{3}He completely due to production of neutrons and tritium through the DD side fusion plasma with equal probability as follows:

$$_1^2D + _1^2D \rightarrow _1^3T(1.01MeV) + _1^1H(3.02 \text{ MeV}) \quad (3)$$

$$_1^2D + _1^2D \rightarrow _2^3He(0.82MeV) + n(2.45 \text{ MeV}) \quad (4)$$
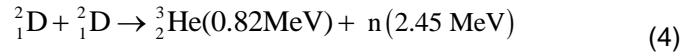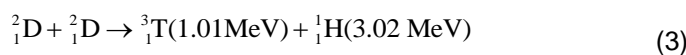
Since tritium does radioactive decay and neutron irradiation influences the reactor equipment, it is necessary to take some methods to limit the radioactivity caused by neutrons in order to prevent from releasing radioactive tritium. Another aneutronic fusion plasma is the plasma of proton with the lithium-6 (p^{6}Li). This plasma:

$$p + _3^6Li \rightarrow _2^4He(1.7MeV) + _2^3He(2.3MeV) \quad (5)$$
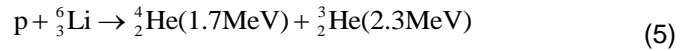
is proposed due to the little load of both components. Helium-3 would regress to plasma in the catalyzed mode and the plasma

$$\frac{d}{dt}(\frac{3}{2}n_iT_i) = P_{ci} + P_{si} - P_{Li} - P_{ie} = 0 \quad (6)$$

provides a very attractive net Q-value. This plasma is not ignitable in low temperatures and it has a very much energy losses in a fusion reactor. Therfore, the study of problems with p^{6}Li plasma in a fusion reactor is significant.

THE PROPERTIES OF P^{6}LI PLASMA

DT fusion reactors inherently encounter with economic and environmental challenges. Therefore, it is strongly emphasized to use a proper alternative among the advanced plasmas. In aneutronic fusion, instead of neutron, most of the energy is released through charged particles. In case of aneutronic plasmas such as D^{3}He, the released tritium and the problems with radioactive wastes decreased. Neutron is produced indirectly through DD and DT side plasmas. D^{3}He fusion reactor suffers from the following disadvantages: (1) Helium-3 is only available through the decay of tritium in proton bomb and also in the future space exploitation programs while just a few countries can afford it or it is produced in the fusion of deuterium-tritium; (2) D^{3}He needs a higher temperature, a more beta and a better containment than DT plasma. p^{6}Li fusion reaction is an aneutronic advanced fuel. Figures 1 and 2 show a cross-section in terms of energy and average reactivity versus ion temperature for different plasmas, respectively. The p^{6}Li fusion plasma has advantages: (1) decreases neutron production; (2) no need for Lithium blanket requirement; (3) reduces tritium inventory; (4) direct electrical conversion; (5) optimum chain plasma features. Unfortunately, it has disadvantages including: (1) high bremsstrahlung radiation; (2) produces indirect radioactive ^{7}Be and ^{11}C; (3) utilizes condensable plasma (^{6}Li); and (4) high-temperature for ignition (Mily, 1981).

ENERGY BALANCE IN P^{6}LI PLASMA

It is necessary in the reactors that the input power be sufficiently low when it is compared to the power output for production of a great net power. The study of the p^{6}Li plasma is important in equilibrium state. The conditions is different for "ideal ignition" and "ignition" cases. In "ideal ignition" which are lower sets for the operating temperature in the plasma. In "ignition" mode is restricted; the pressure, energy confinement time, and temperature for the plasma in stable mode under real condition. The mode of ignition is more practical in this plasma. It is assumed without external power for sustentation of the p^{6}Li plasma. Here, ion and electron energy balance equations reviewed for this plasma. Ion energy balance equation as:

$$\frac{d}{dt}(\frac{3}{2}n_i T_i) = P_{ci} + P_{si} - P_{Li} - P_{ie} = 0 \tag{7}$$

where P_{ci} is the amount of energy transferred from charged particles to ions per unit of time, P_{si} is the injected power, P_{Li} is expended energy of each ion per unit of time and P_{ie} is the rate of energy losses by ions as the follow (Spitzer, 1940):

$$P_{ie} = 7.61 \times 10^{-28} n_e \sum_i \frac{Z_i^2 n_i \ln\Lambda}{\mu_i T_e^{\frac{3}{2}}} \left(1 + \frac{m_e}{m_i}\frac{T_i}{T_e}\right)^{-\frac{3}{2}} \left(1 + \frac{0.3T_e}{m_e c^2}\right)(T_i - T_e) \quad \frac{W}{cm^3} \tag{8}$$

Electron and ion temperature T_e, T_i and the electron rest energy $m_e c^2$ are in eV, m_i is the ion mass ($m_i = \mu_i m_p$, m_p is the proton mass) and density n is in cm^{-3}. The Coulomb logarithm is $\ln\Lambda \approx 31 - \ln(\frac{\sqrt{n_e}}{T_e})$ (Fundamenski and Garcia, 2007). Electron energy balance equation is:

$$\frac{d}{dt}(\frac{3}{2}n_e T_e) = P_{ce} + P_{se} + P_{ie} - P_{Le} - P_B - P_C = 0 \tag{9}$$

In comparison with Equation 8, bremsstrahlung and cyclotron power are the different quantities. P_B is bremsstrahlung radiation power as follows (Nevins, 1998):

$$P_B = 1.62 \times 10^{-32} n_e^2 \sqrt{T_e} \left\{ \sum_i \frac{Z_i^2 n_i}{n_e} \left[1 + 0.7936\frac{T_e}{m_e c^2} + 1.874(\frac{T_e}{m_e c^2})^2\right] + \frac{3}{\sqrt{2}}\frac{T_e}{m_e c^2} \right\} \quad \frac{W}{cm^3} \tag{10}$$

P_C is cyclotron radiation. This can be confined by the magnetic field in an inertial fusion reactor. The calculations show that the amount of $T_i = 800 keV$ and $T_e = 300 keV$ are almost ideal conditions with considered criteria. Fusion power per unit volume produced is:

$$P_f = n_p n_{^6Li} <\sigma\upsilon> E_{fus} = 1.602.10^{-19} \frac{\varepsilon}{(\varepsilon+3)^2} n_e^2 <\sigma\upsilon> E_{fus} \quad \frac{W}{cm^3} \tag{11}$$

where E_{fus} is the released energy (in eV) and $\varepsilon = \frac{n_p}{n_{^6Li}}$. P_f is equal with P_{p^6Li}. Investigations indicate that P_f is maximized for p^{6}Li plasma by assuming $\varepsilon = 3$ with $T_e = 300 keV$ and $n_e = 10^{25} cm^{-3}$. The results show that P_f and P_B increase with high T_e and n_e. Figure 3a displays the ideal T_i is 800 keV. In this state, P_B is minimized. Figure 3b shows that the ideal fuel mixture is $\varepsilon = 3$. In this factors, P_B is more than P_f. Figure 4a shows that P_B reduces with low T_e. Figure 4b indicates that $\frac{P_{ie}}{P_f}$ decreases with T_e and low $\ln\Lambda$.

The investigations show T_i is also important in $\frac{P_{ie}}{P_f}$ value. $\frac{P_{ie}}{P_f}$ reduces with in low T_i. P_B decreases in low T_e and it makes an enhancement in $\frac{P_{ie}}{P_f}$.

CONCLUSION

This study is showed that for the ignition of p^{6}Li fuel in a fusion reactor, two important problems would emerge; the lossed energy and the need for high-temperature electrons and ions. T_i is obtained by the use of $\frac{P_B}{P_f}$. It has been determined that the operation T_i is almost 800 keV. Coulomb logarithmic decreased to $\ln\Lambda = 5$ and improved p^{6}Li plasma performance. In this case, P_B is more than P_f. At high T_e, radiation losses are very much. Calculations show P_B and P_f increase with high T_e and n_e. P_B is minimized with creating appropriate fuel composition. P_B increases with high T_e. Also, T_e and T_i are impressible in $\frac{P_{ie}}{P_f}$.
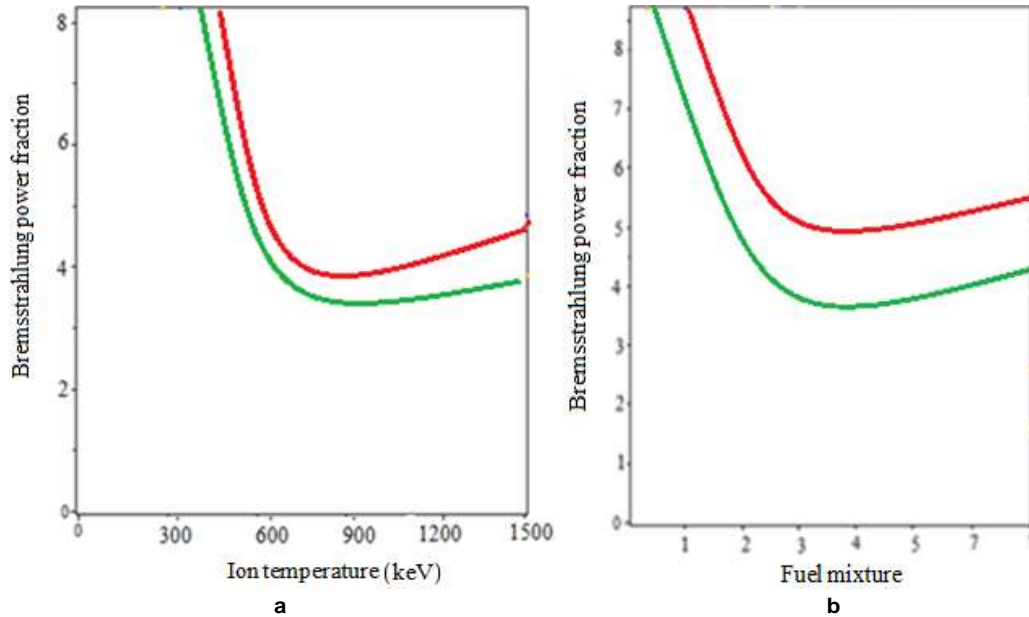
Figure 3. P_B/P_f as a function of (a) T_i (b) $\mathcal{E}$ (red color for $\ln \Lambda = 20$ and green color $\ln \Lambda = 5$).
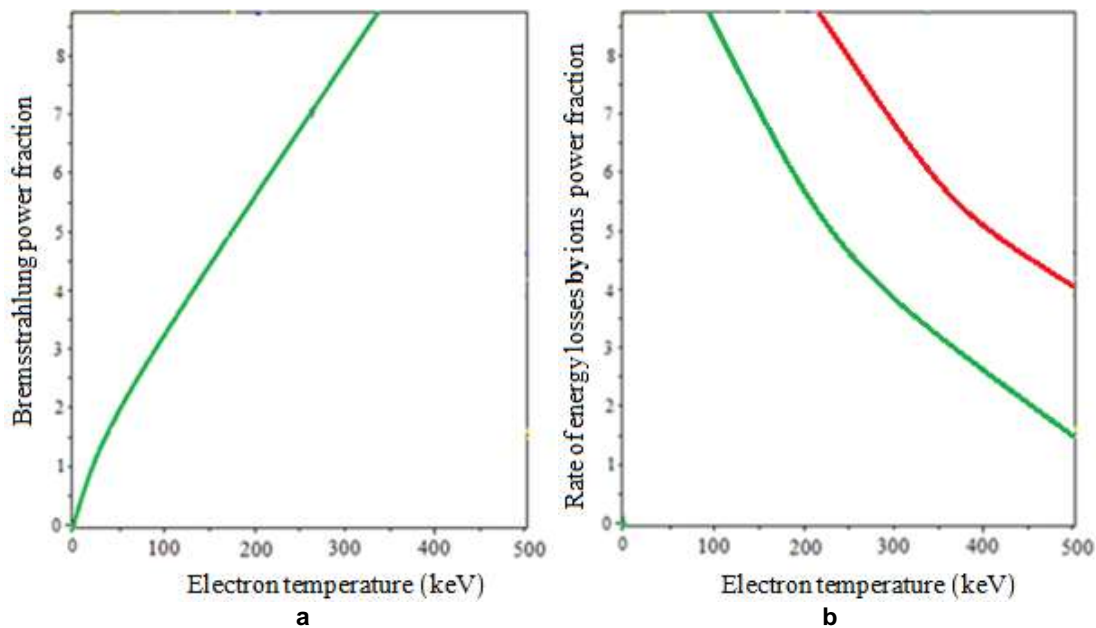
Figure 4. (a) P_B/P_f ; (b) P_{ie}/P_f ; as a function of T_e (red color for $\ln \Lambda = 20$ and green color $\ln \Lambda = 5$).

CONFLICT OF INTERESTS

The authors have not declared any conflict of interests.

REFERENCES

Fundamenski W, Garcia OE (2007). Comparison of Coulomb Collision Rates in the Plasma Physics and Magnetically Confined Fusion Literature. EFDA-JET-R 07:01.

Mily GH (1981). Advance plasma concepts and applications. International Atomic Energy Agency. Third IAEA Technical Committee Meeting and Workshop on Fusion Reactor Design and Technology COO-2218:230.

Momota H, Tomita Y, Nomura Y (1980). An Optimization of Fusion Plasma Parameters. Institute of Plasma Physics, Nagoya university 45:22.

Nevins WM (1998). A review of confinement requirements for advanced fuels. Fusion Energ.17:1.

Spitzer Jr L (1940). The stability of isolated clusters. Mon. Not. R. Astron. Soc. 100:396.

Stott PE (2005). The feasibility of using D–3He and D–D fusion fuels. Plasma Phys. 10:39.

Yu J, Yu G (2009). Status and strategy of fusion materials development in China. J. Nucl. Mater. C 949:386-388.

Full Length Research Paper

Application of Ojih-Okeke modified empirical coronal mass ejection arrival (ECA) model in predicting the arrival time of coronal mass ejections (CMEs)

Ojih Victorial B.[1]* and Okeke Francisca N.[2]

[1]Department of Physics, Federal College of Education (T), Asaba, Delta State, Nigeria.
[2]Department of Physics and Astronomy, University of Nigeria, Nsukka, Nigeria.

Predicting the arrival time of Coronal Mass Ejections (CMEs) with a lower value of average error of the difference between the predicted and the observed transit time is very crucial in space weather forecast. A modified Empirical Coronal Mass Ejection Arrival (ECA) model was proposed, namely, Ojih-Okeke modified ECA model to predict the transit time of twenty eight fast CMEs from the sun to the earth. This is the first time the Ojih-Okeke modified ECA model is being applied in prediction of transit time of CMEs from the sun to the earth. The proposed modified model was tested using data obtained from coronagraph observations of large angle spectrometric aboard, the Solar and Heliospheric Observatory (SOHO/LASCO) CME catalogue from the period of 1997 to 2015. To ascertain the accuracy of the modified model, the three ECA model of Gopalswamy (G2000, G2001, and VG2002) were applied to our data points. Linear regression analyses were carried out on the data points and scatter plots were generated using excel software package. The average error of the difference between the CMEs transit time and models predicted transit time with their fractional errors were 4.27 h and 0.10 for the Ojih-Okeke modified model; 10.36 h and 0.23 for the VG2002 model; 12.93 h and 0.29 for G2001 model; and 14.42 h and 0.32 for the G2000 model. The proposed modified model has proved very effective in prediction of arrival time of CMEs. It is our recommendation that future work on prediction of the arrival time of CMEs be carried out employing our modified ECA model.

Key words: Coronal mass ejections, arrival time, intense geomagnetic storm, observed transit time, earth and phase.

INTRODUCTION

Coronal Mass Ejections (CMEs) are released from the sun's surface into space as massive burst of solar materials consisting of magnetic fields and clouds of plasma. They are the most destructive of all solar events. CMEs may accelerate up to a speed of 3000 kms⁻¹ and gradually propagate through the solar wind, away from

the sun (Yashiro et al., 2001). CMEs are known to be the major cause of severe geomagnetic disturbances which is often referred to as space weather (Zhang et al., 2001; Cheng et al., 2014; Cyr et al., 2000; Mishra and Tripathi, 2005). There are several space weather phenomena which tend to be associated with or are caused by geomagnetic storm. These include Solar Energetic Particles (SEP) events which are hazardous to humans, Geomagnetically Induced Current (GIC) which cause damages to satellites and electrical grid, ionospheric disturbances which may lead to radio and radar scintillation, disruption of navigation by magnetic compass. Therefore, predicting the arrival time of CMEs becomes necessary for this will serve as a practical way of getting advance warning of solar disturbances heading towards the earth, save billions of currency that would have been used to repair or replace damaged satellites and electrical grids, identify communication problems, help high altitude flight management and make provisions for renewable energy sources to protect the earth against black out.

Most researchers have predicted the arrival time of CMEs to 1 AU employing different models. Gopalswamy et al. (2001) developed an Empirical Coronal Mass Ejection Arrival (ECA) model to predict the arrival time of CMEs. From their prediction, they discovered that the average error of the difference between the predicted CMEs arrival time and the observed transit time was 11 h. Owens and Cargil (2004) investigated the three ECA models of Gopalswamy known as G2000, G2001 and VG2002 to predict the arrival time of CMEs to the earth using 35 CME – ICME data obtained from Advanced Composition Explorer (ACE) and Solar and Heliospheric Observatory (SOHO) from November 1997 to April 2001 with CME speed at the sun as input parameter. They asserted that the average error of the difference between the CMEs observed transits time and the predicted 1 AU CMEs arrival time was approximately 11 hrs. Further work was carried out in other to obtain a lower value. Therefore Gopalswamy et al. (2005) later developed an Empirical Shock Arrival (ESA) model to predict the arrival time of CMEs. The average error between the predicted CMEs arrival time and the observed transit time was found to be 12 h. Interestingly, the time interval was 12 h, this increment is not encouraging.

Okeke et al. (2011) used the three empirical models of Golpalswamy (G2000, G2001 and VG2002) to predict the arrival time of twenty-nine Halo CMEs. Their result showed that the average error of the difference between the CMEs observed transit time and the predicted transit time were 15, 12 and 10 h, respectively. They concluded that the errors remained significant and suggested that the model should be enhanced. Mostl et al. (2014) used three geometrical models, namely, Self-Similar Expansion Fitting (SSEF), the Fixed Point Fitting (FPF) and Harmonic Mean Fitting (HMF) to predict the arrival time of 22 CMEs. The SSEF fitting technique allows

flexibility for the CME width in the solar equatorial plane than the FPF or the HMF (extremely wide). The fixed point fitting model assumes a point like CME without any extension in heliocentric longitude. The self-similar expansion model could be seen as a generalization of the fixed point fitting and harmonic mean fitting. All methods share the same assumption of constantly CME speed and direction but differ on the description of the global shape of the CME front. Their results showed that the average error the difference between the CMEs observed transit time and the predicted arrival time was 10.9 h.

Tong et al. (2015) carried out a statistical study of 21 earth directed CMEs using the Graduated Cylindrical Shell and Drag Force Model. The average error of the difference between the predicted and observed transit time was found to be 12.9 h. This high value of 12.9 h is very alarming and disturbing. Carolina et al. (2017) studied the arrival time of eleven coronal mass ejections using microwave radio emissions as a proxy. Their result showed an average error between the observed and predicted transit time to be 11 h for microwaves and 9 h for soft X-ray (S X R). The results of all the aforementioned findings showed that the average error of the difference between the CMEs observed and the predicted transit time is still large. Predicting the arrival time of CMEs with a minimal average error between the CMEs observed and the predicted transit time has been a major issue in the field of Heliophysics.

MATERIALS AND METHODS

The Coronal Mass Ejections data used were procured from Large Angle Spectrometric Coronagraph aboard, the Solar and Heliospheric Observatory (SOHO/LASCO) CME catalog on website (http://cdaw.gsfc.nasa.gov/CMElist/index.html). Only CMEs with initial speed of 900 kms^{-1} and above (fast CMEs) that were associated with geomagnetic storms with Dst≤-100 nT were selected. The geomagnetic storm data were obtained from World Data Centre for geomagnetism Kyoto Japan. Multiple CMEs were avoided as they may lead to CME-CME interaction which may in turn affect the transit time. The CMEs selected were Halo CMEs, it has been established that Halo CMEs are the most geo-effective having ability to cause geomagnetic storm. In order to ascertain the accuracy of the model, the three ECA model of Gopalswamy were also applied to the data points.

Theory of Ojih-Okeke modified ECA model

The authors assumed that: (1) fast CMEs undergo three phases, as they travel from sun to earth: a deceleration which ceases before 0.1 AU, a constant speed propagation until about 0.45 AU and a gradual deceleration to 1 AU; (2) CMEs travel with solar wind speed from 0.45 to 1AU. The transit time of CMEs from the sun to the earth is given by:

$$\tau = \frac{-U+\sqrt{U^2+2a_1\,d_1}}{a_1} + \frac{d_2}{\sqrt{U^2+2a_1\,d_1}} + \frac{-W+\sqrt{W^2+2a_2\,d_3}}{a_2} \tag{1}$$

where U is CMEs initial speed, W is the solar wind speed, d_1=0.08AU, d_2= (0.45AU-0.08AU), d_3= (1AU-0.45AU), a_1= 10^{-3} (0.0054U-2.2) and a_2= 10^{-3} (0.0054W-2.2).

Theory of Gopalswamy et al. (2000) model: Constant acceleration or deceleration

The author assumed that the acceleration was constant between the sun and IAU so that the total effective interplanetary acceleration (α_1) undergone by an interplanetary coronal mass ejection (ICME) is:

$$a_1 = \frac{V(1AU) - U}{\tau}$$

where V (IAU) is the ICME speed at IAU (1 AU, U is astronomical unit) and U is the CME initial speed.

The linear fit to data plot gave an empirical for the effective acceleration $a_1 = 1.41 - 0.00035U$. To improve the model by minimizing the projection effects in determining the initial speed of the CMEs, the author used the archival data from spacecraft in quadrature and this led to an improved formula of $a_2 = 10^{-3}(2.193 - 0.0054U)$.

This can then be used in the kinematic equation:

$$S = U\tau + \frac{1}{2}a_2\tau^2$$

The transit time (τ) of the CMEs from sun to earth is given by:

$$\tau = \frac{-U + \sqrt{U^2 + 2a_2 S}}{a_2} \tag{2}$$

where U is the CMEs initial speed, α_2 is acceleration and S is the distance between the sun and earth.

Theory of Gopalswamy et al. (2001) model: Cessation of acceleration before IAU

The model assumes that ICME acceleration ceased at a heliocentric distance of 0.76 AU for all CMEs irrespective of their initial speed. Therefore, the total transit time from sun to IAU is the sum of the travel time to 0.76 AU at constant acceleration, and the travel time from 0.76 AU to IAU at constant speed.

$$\tau = \frac{-u + \sqrt{u^2 + 2a_2 d}}{a_2} + \frac{IAU - d}{\sqrt{U^2 + 2a_2 d}} \tag{3}$$

where a_2 is an effective interplanetary acceleration that was derived empirically from quadratic observations of CMEs, U is initial speed of CMEs and d is the acceleration cessation distance (0.76 AU).

Theory of Vrsnak and Gopalswamy (2002) model: Aerodynamic drag

The model was proposed for estimating the ICME transit time when the only force acting upon the ICME in interplanetary space is the aerodynamic drag. They assumed that the drag force was linearly proportional to the relative velocity.

The equation of motion of an ICME at some heliocentric distance R (R=$\frac{r}{r_s}$, where r is heliocentric radius and r_s is solar radius given by:

$$\frac{dV}{d\tau} = \alpha R^{-\beta}(V - W)$$

where α and β are constants that parameterize the drag as a function of distance and speed is given by Sheeley et al. (1997) as;

$$W(R) = W_0 \sqrt{1 - e^{\frac{2.8 - R}{8.1}}}$$

where W_0 is the asymptotic solar wind speed ($W_0 = 400$ kms^{-1}). Writing this in terms of R gives:

$$\frac{dV}{dR} = r_s \alpha R^{-\beta}\left(1 - \frac{W}{V}\right)$$

Numerical integration from the low corona (R=10), where it is assumed that V=U to IAU then gives V(R), V is CMEs speed at R = 10.

$$\tau = \frac{r_s R}{V} + \frac{10 r_s}{U} \tag{4}$$

Equations 1, 2, 3, and 4 were applied to the CMEs data to calculate the predicted arrival time for each model. The difference between the CMEs observed transit time and the model's predicted transit ($\Delta\tau$) were calculated. The average error and fractional error of the difference between the CMEs predicted transit and observed transit time for each model was calculated.

RESULTS

The average error between the observed and predicted transit time and fractional errors are shown in Table 1. Scatter plots of CMEs predicted transit time as function of CMEs initial speed were generated for each model.

DISCUSSION

The model equations were applied to the CMEs data. The difference between the CMEs predicted and observed transit time ($\Delta\tau = \tau_{mod} - \tau_{obs}$) were calculated for each model. The average error between the CMEs observed and the predicted transit time and the fractional error for each model were also calculated. Table 1 shows the summary of the average error and fractional error between the CMEs observed and predicted transit time ($\Delta\tau$) and fractional error of twenty eight fast coronal mass ejection events associated with intense geomagnetic storm observed from the period of 1997 to 2015. The average error and fractional error of the difference between the CMEs observed and the predicted transit time for Gopalswamy 2000 (G2000) model were 14.42 h and 0.33. This result obtained for the G2000 model is in close agreement with the result of Okeke et al. (2011) who obtained the average error between the CMEs observed and predicted transit time of 14.83 h and fractional error of 0.57.

The average error of the difference between the CMEs observed and the predicted transit time and the fractional

Table 1. Summary of the average error and fractional error in the model.

Model	$<\Delta\tau>$ h	$<\Delta\tau/\tau>$
Ojih-Okeke modified model	4.27	0.10
VG 2002	10.36	0.23
G2001	12.93	0.29
G2000	14.42	0.33

The table presents the summary of the average error and fractional error obtained in the models. Column 1 represents the empirical models, column 2 is the average error of the difference between the CMEs predicted and observed transit time ($\Delta\tau$) and column 3 is the fractional error between the CMEs predicted and observed transit time in each model'.
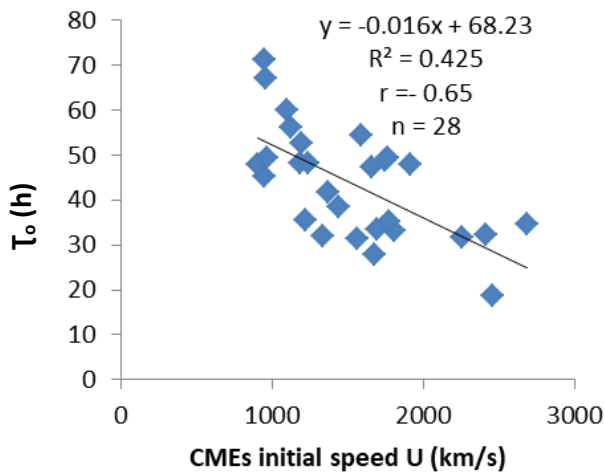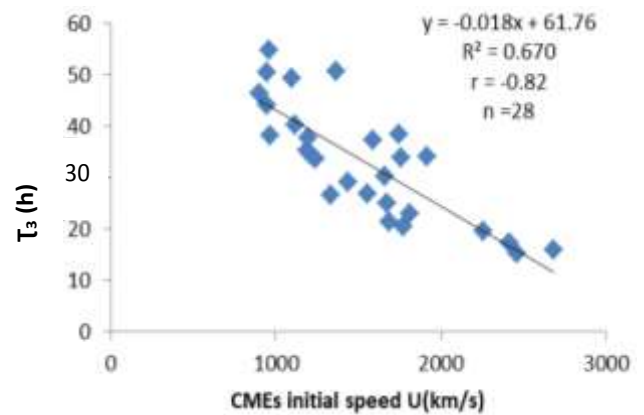

Figure 1. A plot CMEs observed transit time as a function of CMEs initial speed.
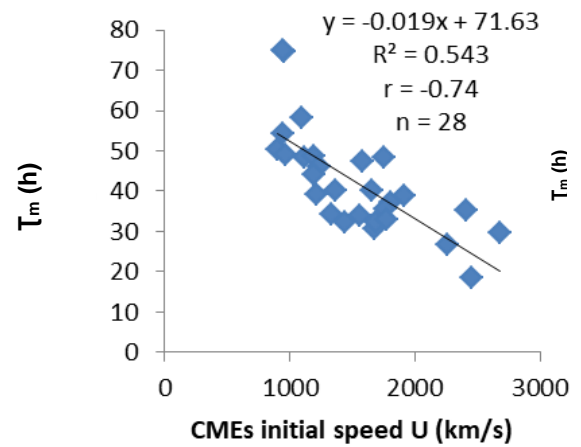
Figure 2. A plot CMEs predicted transit time as a function of CMEs initial speed for Ojih-Okeke modified model.

error obtained for Gopalswamy 2001 (G2001) model were 12.93 h and 0.29, respectively. The average error between the CMEs predicted transit time and the observed transit time obtained for the Vrsnak and Gopaswmy, 2002 (VG2002) is 10.36 h while the fractional error is 0.23. The average error between the CMEs predicted and observed transit time obtained for the Ojih-Okeke modified model was 4.27 h with fractional error of 0.10. The error in Ojih-Okeke modified model is likely traceable to geometrical effects. According to Carolina et al. (2017), CMEs is a curved 3-D structure, the measured arrival time depends on which part of CMEs is being sampled and also CMEs become deformed in the interplanetary medium with an elongation taking place in a direction perpendicular to the principal direction of the motion.
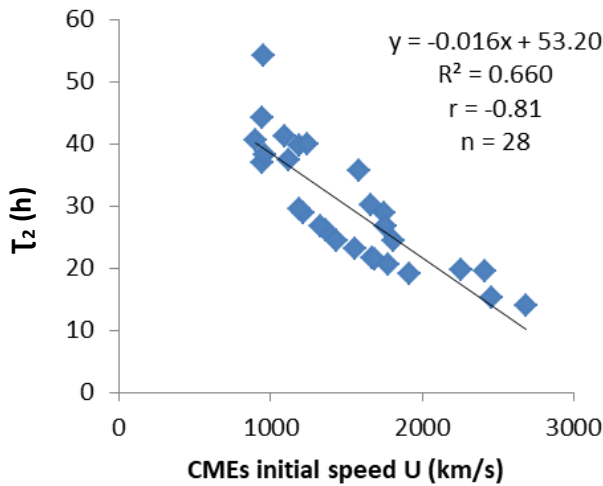
Figure 1 show a scatter plot of the CMEs observed transit time as a function of CMEs initial speed. The linear correlation coefficient obtained from the scatter plot is -0.65 the negative correlation shows that as speed increases, time decreases. Figures 2, 3, 4 and 5 show the scatter plots of CMEs predicted transit time as function of
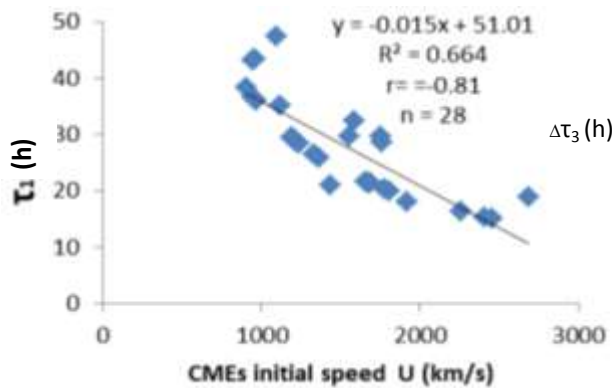

Figure 3. A plot of CMEs predicted transit time as a function of CMEs initial speed for VG2002 model.

CMEs initial speed for Ojih –Okeke modified model, VG2002 model G2001 model and G2000 model. The values of the linear correlations coefficients obtained from the scatter plots are -0.74 for the Ojih-Okeke modified
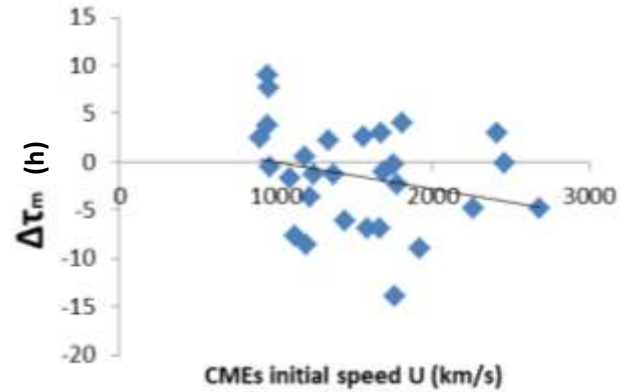
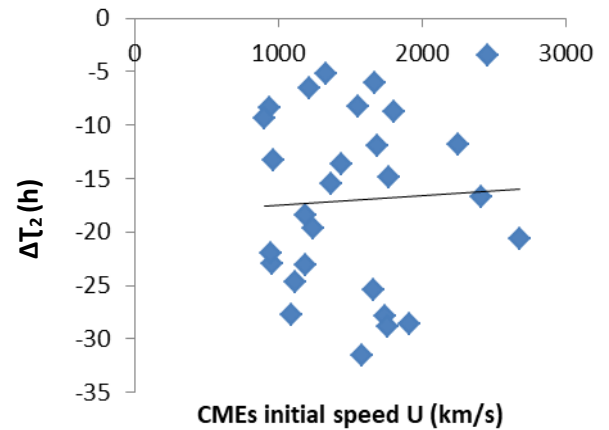Figure 4. A plot of CMEs predicted transit time as a function of CMEs initial speed for G2001model.

Figure 5. A plot CMEs predicted transit time as a function of CMEs initial speed for G2000 model.

Figure 6. A plot of the difference between the CMEs predicted and observed transit time as a function CMEs initial speed for Ojih-Okeke modified model.

Figure 7. A plot of the difference between the CMEs predicted and observed transit time as a function CMEs initial Sp speed for VG2001 model.

Figure 8. A plot of the difference between the CMEs predicted and observed transit time as a function CMEs initial speed for G2002 model.

model; -0.82 for VG2002 model; -0.81 for the G2001 model and -0.81 for G2000 model. These values of linear correlation coefficients obtained from the four models depict that there exist a strong correlation between CMEs transit time and CMEs initial speed.
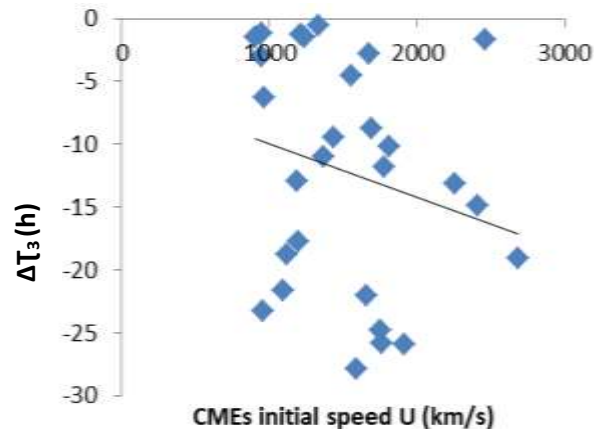
Figures 6, 7, 8 and 9 show the scatter plots of the difference between the predicted transit time and the observed transit time ($\Delta\tau$) as function of CMEs initial speed for Ojih-Okeke modified model, G2001 model, VG2002 model, and G2000 model, respectively. The G2000 model, G2001 model and the VG2002 model predict all the 28 events corresponding to 100% earlier than observed. It is obvious that the G2000, G2001 and VG2002 models underestimate the CMEs transit time as the plots show large negative distribution of $\Delta\tau$ Hence, the need for the development of a modified model. The modified model predict 18 events out of the 28 events
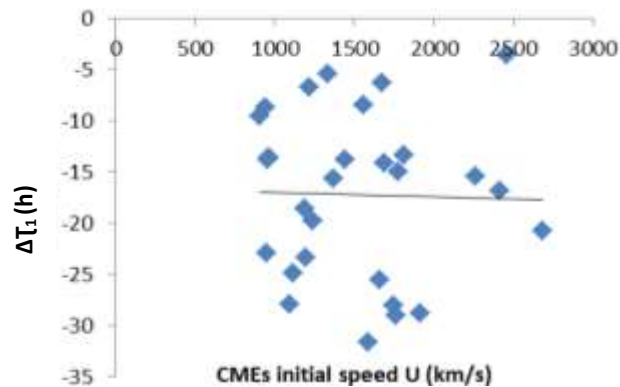
Figure 9. A plot of the difference between the CMEs predicted and observed transit time as a function CMEs initial speed for G2000 model.

corresponding to 64.29% earlier than observed and 10 events corresponding to 35.71% later than observed. Although there are still some slight deviations between the predicted transit time and the observed transit time as observed from the plots. The cause of these slight deviations was attributed to geometrical effect. Geometrical effects due to two reasons, firstly CME is a curved 3-D structure and the measured arrival time depends on the part of the CME that is being sampled by SOHO coronagraph. Secondly, CME becomes deformed in the interplanetary medium with elongation taking place in a direction perpendicular to the principal direction of the motion.

Some researchers attributed the error in CMEs predicted transit time to projection effects. Owens and Cargil (2004) in their analysis of the cause of error asserted that projection effect has no significant difference between the values obtained with projection effects and when projection was removed.

Conclusion

The Ojih-Okeke modified ECA model was applied to predict the transit time of 28 fast CMEs associated with intense geomagnetic storm (Dst≤-100 nT) obtained from the period of 1997 to 2015. Inferences drawn from our results show that the average error of the difference between the CMEs observed transit time and the modified model's transit time and fractional error were much lower than those obtained from the earlier models. Comparing the results obtained from the four models, the Ojih-Okeke modified model proved the most accurate model for predicting the arrival time of fast CMEs. This is the first time the modified model is being applied to predict the transit time of CMEs from the sun to the earth. It is therefore recommended that future work on prediction of the arrival time of CMEs be carried out employing Ojih-Okeke modified ECA model.

CONFLICT OF INTERESTS

The authors have not declared any conflict of interests.

ACKNOWLEDGEMENTS

REFERENCES

Carolina SM, Karl L, Gerard T (2017). Microwave radio emission as a proxy for coronal mass ejection arrival speed in predictions of interplanetary coronal mass ejections at IAU. Space Weather Space Climate J. 7:A2.
Cheng L, Shen YZ, Bin A, Ye MP, Wang S (2014). Full Halo coronal mass ejections arrival at the earth. http:// space.ustc.edu. Cn /dreams/.fhcmes/.
Cyr OC, Raymond JC, Thompson BJ, Gopalswamy NK, Kahler SK, Lara N, claravella A, Romol N, Oneal R (2000). SOHO and Radio observation of CME shock Wave. Geophys. Res. Letters J. 27(10):1439-1442.
Gopalswamy N, Lara A, Lepping RP, Kaiser ML, Berdichevsky D, Cyr OC (2000). Interplanetary acceleration of coronal mass ejections. Geophys. Res. Lett. J. 27:145.
Gopalswamy N, Alejandro L, Russel A H (2001). Predicting the I-AU arrival times of coronal mass ejections. Geophys. Res. J. 106(A12):29, 207-209, 217.
Gopalswamy N, Alejandro L, Yashiro S, Kaiser ML, Howard RA (2005). An empirical model to predict the 1-AU arrival of interplanetary shocks. Adv. space res. J. 36(12):2289-2294.
Mishra AP, Tripathi RM (2005). Characteristics features of CMEs with respect to their source region. Proceeding of the 29th International Cosmic Ray Conference, Pune, India 1:149.
Mostl CK, Amla JR, Hall PC, Liewer EM, Jong RC, Colaninno AM, Galvin AB (2014). Connecting speeds , directions and arrival time of 22 Coronal Mass Ejection from the Sun to 1AU. Astrophysi. J. V5/2/11.
Okeke FN, Okpala KC, Akaogu V (2011). Predictions of the arrival time of Coronal Mass Ejection (CME) and its contributions to major Geomagnetic storms. Nig. J. Space Res. 10:217-230.
Owens M, Cargil P (2004). Predictions of the arrival time of Coronal Mass Ejection at IAU: an analysis of the causes of errors.
Sheeley NR, Wang YM, Hawley SH, Bruckner GE, Dere, KP, Howard RA, Koomen MJ, Korendyke CM, Michels DJ, Paswaters SE, Socker DG, St. Cyr OC, Wang D, Lamy PL, Liberia A, Schwenn R, Simnett GH, Plunkett S Biesecker DA (1997). Measurements of the flow speed in the corona between 2 and 30 r$_s$. Astrophys. J. 484:472.
Tong S, Yikang W, Linfeng W, Xin C, Mingde D, Jie Z (2015). Predicting the arrival time of coronal mass ejection with the graduated cylindrical shell and drag force model. Astrophys. Res. letters J. 806:2.
Vrsnak B, Gopalswamy N (2002). Influence of aerodynamic drag on the motion interplanetary ejecta. J. Geophys. Res. 107:10.1029/2001/JA 000120.
Yashiro SN, Gopalswamy GM, Cyr OC, Plunkett SP, Rich NB, Howard RA (2001). A catalog of white light coronal mass ejections observed by the SOHO Spacecraft. J. Geophys. Res. 109(A):7105.
Zhang J, Wang T, Zhang C, Liu Y, Nitta N, Slater GL, Wang J (2001). Flare-CME events association with a super activeregion recent insight into the Physics of the Sun and heliosphere: Highlights from SOHO and other space missions. Pal Brekke (Eds), Proceedings of IAU Symposium. P 203.

International Journal of Physical Sciences